IEEE Access
Multidisciplinary | Rapid Review | Open Access Journal

Received 12 August 2022, accepted 1 September 2022, date of publication 5 September 2022, date of current version 15 September 2022.

Digital Object Identifier 10.1109/ACCESS.2022.3204671

RESEARCH ARTICLE

PI Controller for Hybrid Biomass- Solar Photovoltaic- Wind in Microgrid: A Case Study of Mersing, Malaysia

SAIDATUL HANEEN BADRUHISHAM, MOHD SHAHRIN ABU HANIFAH, (Member, IEEE), SITI HAJAR YUSOFF, (Member, IEEE), NURUL FADZLIN HASBULLAH, AND MASHKURI YAACOB, (Life Senior Member, IEEE)

Department of Electrical and Computer Engineering, International Islamic University Malaysia (IIUM), Kuala Lumpur 53100, Malaysia

Corresponding author: Mohd Shahrin Abu Hanifah (shahrin@iium.edu.my)

This work was supported by the Ministry of Higher Education Malaysia under Fundamental Research Grant Scheme FRGS19-067-0675.

ABSTRACT Renewable energy (RE) is alternative energy to replace fossil fuels in electric power generation and has evolved into microgrid technology. Integration of RE has caused voltage stability issues in the power system. Reports in earlier studies have included three voltage control methods such as Model Predictive Control (MPC), Proportional Integral (PI) controller, and negative feed-forward voltage control implemented to ensure the voltage stability of microgrids. However, very few research reports apply voltage control in hybrid biomass (BM)-solar photovoltaic (PV)-wind microgrid, choosing only to focus on energy management, economic analysis, and best sizing. For this reason, the main objective of this paper is the integration of a hybrid BM-Solar PV-Wind off-grid microgrid comprising PI controller as the voltage control based on an actual input database at a location in a small rural town named Mersing in Malaysia. Additionally, this paper also intends to illustrate the implemented efforts to support the voltage stability of the system in Mersing. PI controller with a harmonic filter voltage controller is implemented in this study to reduce the total harmonic distortion (THD) percentage. Concurrently the measured THD voltage and current at each RE and distribution line show a percentage below 10%. It is thus shown that a hybrid BM-Solar PV-wind microgrid is stable, especially for distribution lines, according to harmonic standards in the electricity supply application book by the local electricity provider Tenaga Nasional Berhad (TNB). Indeed, a PI controller with a harmonic filter has proven as an effective method for controlling the voltage instability in this study.

INDEX TERMS Hybrid renewable energy, Mersing Malaysia, off-grid microgrid, proportional integral controller, total harmonic distortion, voltage control.

NOMENCLATURE

ACRONYMS

BM	Biomass.
DG	Distributed generation.
DMC	Discrete-time sliding control.
EFB	Empty fruit bunch.
HPSHS	High pressure superheated steam.
MMD	Malaysian Meteorological.
MPC	Model predictive controller.
MPPT	Maximum power point tracker.
NASA	National aeronautics and space administration.
PMSG	Permanent magnet synchronous generator.
PV	Photovoltaic.
RE	Renewable energy.
RSC	Robust servomechanism control department.
SDG	Sustainable Development Goal.
THD	Total harmonic distortion.
TNB	Tenaga Nasional Berhad.
UN	United Nation.
VSI	Voltage source inverter.

The associate editor coordinating the review of this manuscript and approving it for publication was Ahmed Mohamed.

I. INTRODUCTION

Environmental issues such as global warming and unexpected natural disaster occurrence have diverted the focus of researchers toward renewable energy. According to the National Aeronautics and Space Administration (NASA) report, global temperature has increased by 1.18°C per year and caused a shrinking ice sheet by 428 billion metric tons per year [1]. These phenomena have happened due to human activities such as deforestation, burning fossil fuels to produce electricity for consumers, and transportation activities that also burned fossil fuels. Thereupon, researchers currently have embarked on extensive research on RE to replace fossil fuel to reduce carbon emissions and achieve the seventh (affordable and clean energy) goal in the Sustainable Development Goals (SDG) proposed by the United Nations (UN). Renewable energy (RE) such as solar, wind, and biomass have become commonly used energy in the industry to supply electricity due to their sustainability and being environmentally friendly. Their integration in power systems has evolved into microgrid technology.

A microgrid is an interconnected network of distributed generation (DG), storage devices, and load [2], [3], [4], [5]. The microgrid can be connected to the grid or operated in off-grid mode [6], [7]. Grid-connected microgrid operates in the presence of the grid that may have sufficient power and thus ensure grid stability and reliability [8]. Meanwhile, off-grid or islanded mode runs without the presence of a grid. This type of microgrid mode needs a control strategy to ensure its stability and reliability in power quality due to short circuits, power reduction, virtual impedance, and output voltage mismatch between converters caused by the absence of a primary source (grid) [9]. The microgrid can supply eco-friendly energy with power loss reduction in transmission lines and improve power system reliability [10], [11].

Solar photovoltaic (PV) and wind are two renewable energies growing fast due to cost reduction over the past few years and are easily harnessed from their resources. However, these two renewable energies are intermittent and unpredictable. Consequently, biomass (BM) energy has become an alternative source as a backup to the solar and wind supply. In the case of Malaysia, it is possible to generate biomass energy because it has abundant biomass resources [12]. Incidentally, renewable energy integration in microgrids has caused many problems such as voltage instability, low power quality, storage needs, and re-synchronization with the primary grid because of their intermittent and unpredictable sources [13].

For this reason, power quality is a crucial issue in the microgrid, and one of the common problems in a microgrid is voltage instability [14]. The microgrid systems' stability and reliability depend on voltage regulation, especially with more DG interconnection. This paper will present the voltage stability of the renewable energy microgrid system in Malaysia's case study. Microgrid imbalance causes a detrimental effect on equipment malfunction that can cause sudden tripping of the circuit breaker. Besides, power quality will suffer losses and unstable conditions [15]. These problems will result in frequent system blackouts and raise consumer dissatisfaction. It is therefore imperative that these problems are resolved to ensure system stability and reliability.

On an off-grid connected microgrid, the inverter can support voltage regulation within the network, in which the voltage output will directly affect the power quality [16]. On the other hand, the inverter also determines the system's voltage stability as it acts as the bridge between the DC and AC bus [17]. The popular solution to compensate for the voltage unbalance is by implementing the active power filter or voltage control strategy for the inverter. Reference [16] proposed a negative voltage feed-forward control method to improve dynamic voltage responses on sudden load variation [16]. Model Predictive Controller (MPC) for voltage control was proposed by [18] for single-phase off-grid connected microgrids. This control strategy intends to support a constant voltage across a range of load types, and the complexity of the control is the limitation of this control.

Moreover, [19] describes the development of a stand-alone split dc bus Voltage Source Inverter (VSI) control strategy. The control technique employs a combination of discrete-time sliding control (DSMC) with Robust Servomechanism Control (RSC) [19]. This technique aims to achieve low steady-state error, low total harmonic distortion (THD), and rapid transient response under various load disturbances and unbalance [19]. On the other hand, a harmonic power filter also has been proposed by [20] to reduce the harmonics and enhance system stability. A power harmonic filter includes a resistance (R), an inductance (L), and a capacitor (C). An RLC is connected between the inverter and AC bus microgrid. The result shown in [20] concludes that a harmonic power filter can reduce the THD of the system.

This paper presents a hybrid BM-PV-wind in an off-grid connected microgrid for Mersing, Malaysia case study. Previously, research on hybrid biomass-solar PV-wind had been conducted but was only focused on energy management, optimal sizing, and economic analysis [21], [22], [23], [24], [25], [26], [27]. The researchers in [5] proposed a voltage control of biomass-solar PV-wind microgrid using general parameters from previous research. However, the author(s) did not consider each renewable energy's power output and current THD. In this study, Malaysia input was implemented into the same model in [5] with the observation of power output and the THD value of every renewable energy. In addition, the PI controller is also applied as a voltage controller in this system. They are seeing that the benefit of the PI controller, such as its simplicity, fast transient response, and ability to produce excellent voltage stability, made it a primary feature from other voltage controls. The hybrid BM-PV-wind microgrid architecture is built based on [5], but the input database is on the real Malaysia Meteorological Department (MMD) data. This research aims to implement a Malaysia data case study in a hybrid BM-PV-wind microgrid in an off-grid connection and observe the voltage stability with a PI controller by checking the power output, system voltage, and current THD value. The main contribution of this paper

successfully controls the voltage instability of the proposed microgrid system with PI controller and power harmonic filter.

The structure of the paper is as follows; modeling the solar, wind, biomass, components, and PI controller discussed in section 2. Sections 3 and 4 discuss the result obtained, research discussion, conclusion, and future recommendations.

II. METHODOLOGY

Fig.1 shows the proposed integration of a hybrid BM-Solar PV-Wind microgrid consisting of AC and DC buses. The solar supply links with the DC bus through the DC/DC converter (boost converter) with MPPT to increase the DC voltage and connect to the AC bus. The PI controller controls the inverter to stabilize DC voltage conversion. Wind and biomass energy systems are connected to the AC buses via a generator that converts mechanical energy to electrical energy.

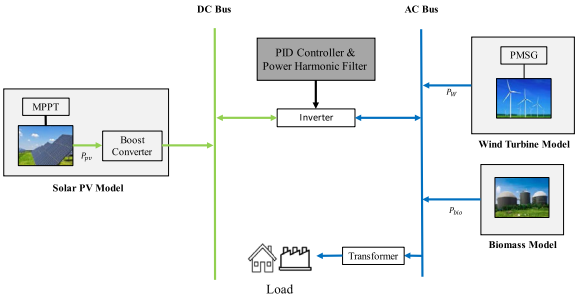

FIGURE 1. Proposed hybrid BM-Solar PV-Wind microgrid [5].

TABLE 1. Renewable energy control strategy.

Distribution Generator (DG)	Component	Control method
Solar	Boost converter	Maximum Power Point Tracker (MPPT)
	Inverter	PI controller
Wind	PMSG	-
	Inverter	PI controller

Each renewable energy has its control strategy in its modeling except for biomass generation because its input is predictable. Thus, the voltage and current for biomass are always stable without any voltage control. Table 1 shows the overall control strategy for each renewable energy design in this system. Additionally, the input database used for solar, and wind is based on the actual data at Mersing from MMD. Fig. 2 shows the input database's location for the Malaysia case study and Fig. 5 shows the methodology overview of this paper. The next subtopic presents the discussion on the modeling of each renewable energy and its control such as solar PV, MPPT, wind, biomass, and PI controller which were designed individually based on the reference paper. Thus, subtopics A, B, C, D, and E discuss the RE modeling. Lastly, subtopic F discusses the integration of hybrid biomass-solar PV-wind in a microgrid application

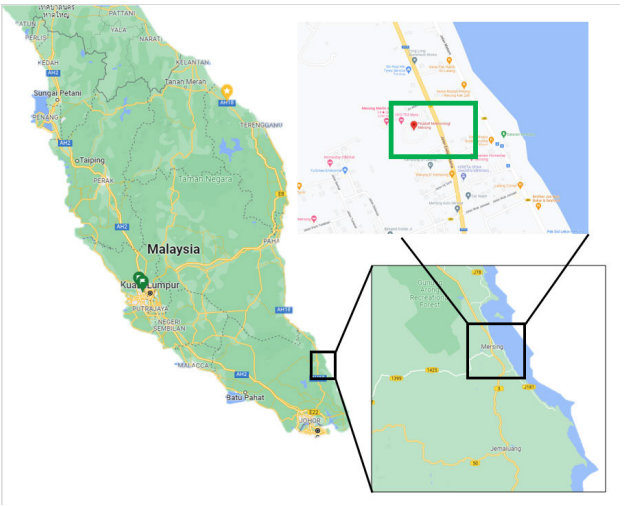

FIGURE 2. Input database location in Mersing, Malaysia [28].

A. SOLAR MODELING

Solar generation solely depends on the temperature and irradiation of the surrounding. The output power of the solar photovoltaic can be calculated as [22]

$$P_{pv} = n_{pv}\,(G, T)\,AG(t) \tag{1}$$

where n_{pv} is the efficiency of solar panels, G is solar radiation in W/m^2, T is the temperature (°C), A is the solar panel area (m^2), and t is the time (s) [21]. The modeling of the solar PV system uses real input daily temperature data from MMD at Mersing in 2018.

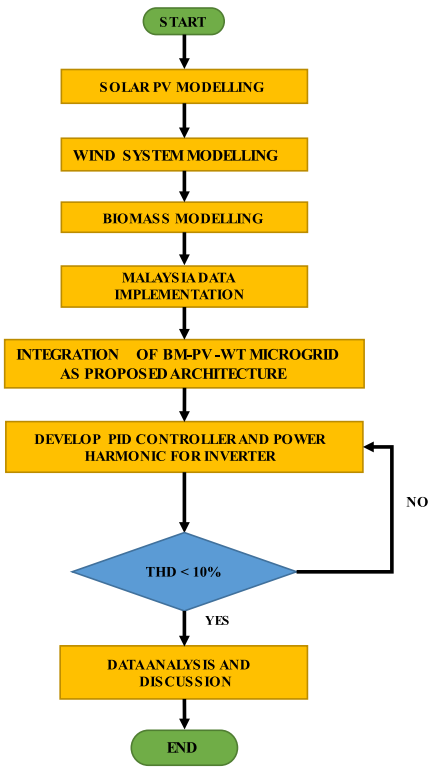

FIGURE 3. Methodology overview.

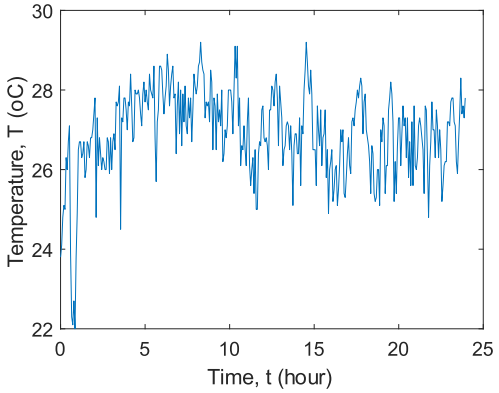

FIGURE 4. Solar temperature in Mersing 2018 [29].

Fig.4 shows the temperature input database used in the simulation. The data in Fig. 4 shows the simplified temperature data for 2018 because the data set holds 365 variable values, which causes a longer simulation time. Thus, the data were compressed into 24 hours to observe the solar output for a day with average solar temperature of 27°C. Fig.5 shows the irradiance considered in the system with average 800 W/m^2 irradiance at Mersing.

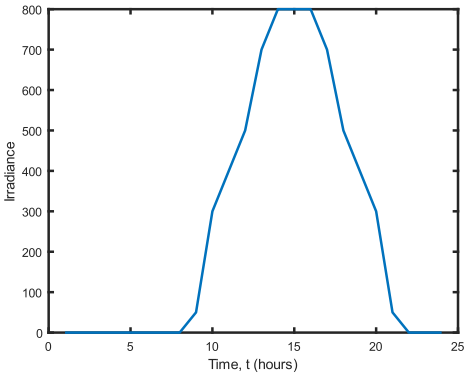

FIGURE 5. Solar irradiance.

The solar modeling in Matlab/Simulink used the available block with temperature, radiation, and number of solar panels as the variables. Table 2 depicts the variables considered in this study.

TABLE 2. Variables of solar PV modelling.

Variable	Value
Temperature	Fig.3
Solar radiation	800 W/m^2
Parallel string	24
Series-connected module per string	7

B. MAXIMUM POWER POINT TRACKER (MPPT)

The Maximum Power Point Tracker (MPPT) is used to operate the photovoltaic panel at its peak power output regardless of the irradiance, temperature, or load current variation [30]. This study used the perturb and observe (P&O) method because of the design's simplicity and good performance [31]. Fig. 6 illustrates the P&O MPPT technique flow chart. The duty cycle (D) is directly proportional to the voltage and power of the solar PV. If the power output and voltage increase, the duty cycle (D) also increase in the same direction otherwise D will decrease with a step (ΔD). The iteration will continue entil maximum power point is reached [31].

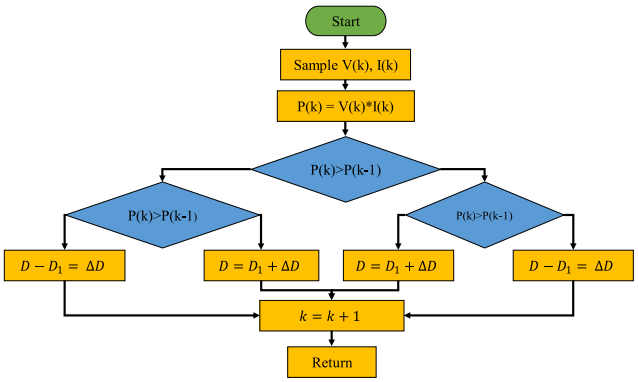

FIGURE 6. Flow chart of P&O MPPT technique [31].

The algorithm of P&O compares the power and voltage of time (k) to a single sample (k-1) [32]. A small voltage perturbation alters the solar panel's output. If the power output increases, the voltage perturbation continues in the same direction. Besides, the duty cycle (D) also increases as D is directly proportional to the voltage and solar PV power output [31], [32]. However, if the delta is negative, the MPP is a long distance away, and the iteration will continue until it reaches the maximum power point [31], [32].

C. WIND MODELING

Wind speed is crucial in producing high power output in wind turbine generation. The wind turbine power output can be expressed as [33]

$$P_W = 1/2C_P(\lambda, \theta)\,\rho A v^3 \tag{2}$$

where; C_P is power coefficient of the wind turbine, λ is tip speed ratio, θ is pitch angle, ρ is air density. A is the swept area, v is wind velocity [33].

$C_P(\lambda, \beta)$, power coefficient of wind turbine is the ratio of the extracted by the wind turbine relative to energy available in wind stream can be expressed as [34]

$$C_p = C_1(C_2/\lambda_i - C_3\beta - C_4\beta^x - C_5)\exp(-C_6/\lambda_i) \tag{3}$$

where β is blade pitch angle and C_1, C_2, C_3, C_4, C_5, C_6 is a constant value [34].

The tip speed ratio also can be expressed as [34]

$$\lambda = \omega R/v \tag{4}$$

where ω is rotor speed in rad/s.

Table 3 shows the parameter in wind modeling based on the calculation from Eqs 2 – Eqs. 3. Fig. 7 shows the wind speed real input database from MMD at Mersing in 2018. The data

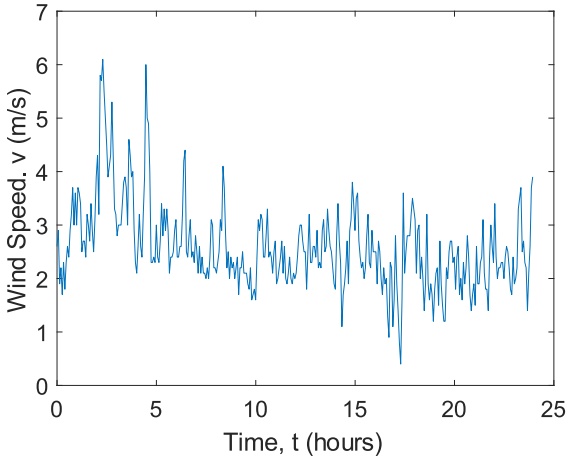

FIGURE 7. Wind speed at Mersing (2018) [29].

TABLE 3. Wind design parameter.

Parameter	Value
λ	8.1
R	25 m
C_1	0.5
C_2	116
C_3	0.4
C_4	0
C_5	5
C_6	1

from Fig. 7 is simplified data to 24 hours same as solar temperature. The average wind speed from the graph is 2.6 m/s which is quite low for wind turbine generation. However, Permanent Magnet Synchronous Generator (PMSG) aims to convert the wind turbine's mechanical energy to electrical energy, operating at low speed to elevate the wind turbine efficiency [34]. The design of PMSG in Matlab/Simulink is by using the available block in library.

D. BIOMASS

Biomass energy can be a reliable backup for other unpredictable renewable energy sources in the power system. Empty Fruit Bunches (EFB) are used as the fuel resource in this study. For prediction, the amount of heat extract from the combustion process can be calculated as [35]

$$Q_c = m_f \times \mathrm{CV_f} \times \eta_{\mathrm{boiler}} \tag{5}$$

where, m_f is the feedstock flow rate (kg/s), CV_f is the feedstock calorific value (MJ/kg), and η_{boiler} is boiler thermal efficiency [35].

The mass flow rate of the High-Pressure Superheated Steam (HPSHS) can be expressed as [35]

$$Q_c = m_{\mathrm{HPSHS}} \left[\begin{array}{l} C_{\mathrm{pb}} \left(T_{\mathrm{sat}} - T_{\mathrm{BWF}}\right) + \Delta H_{\mathrm{vap}} + \\ \left(h_{\mathrm{sup}} - h_v\right) \end{array} \right] \tag{6}$$

where, C_{pb} is water specific heat capacity, T_{sat} is the saturated temperature of steam, T_{BWF} is the temperature of boiler feed water, ΔH_{vap} is the standard enthalpy of vaporization water, h_{sup} is specific enthalpy of HPSHS, and h_v is specific enthalpy of saturated steam [35].

TABLE 4. Biomass modelling parameter [35].

Parameters	Value
Specific heat capacity of water, C_p	4.187 kJ/kg°C
Saturated temperature of steam, T_{sat}	264 °C
Temperature of boiler feed water, T_{BWF}	105 °C
Standard enthalpy of vaporization water, ΔH_{vap}	1639.6 kJ/kg
Specific enthalpy of HPSHS, h_{sup}	3433.7 kJ/kg
Specific enthalpy of saturated steam, h_v	2794.2 kJ/kg
Feedstock flow rate, m_f	0.3208 kg/s
Feedstock calorifiv value, CV_f	8.5 MJ/kg
Boiler thermal efficiency, η_{boiler}	85%

HPSHS generated on an annual basis can be expressed as

$$\mathrm{HPSHS_{ACC}} = m_s \times 60 \times 60 \times \text{operation hour} \tag{7}$$

Electricity generation capacity (MW) can be calculated as [35]

$$E_{\mathrm{cap}} = (\mathrm{HPSHS_{ACC}} \times h_{\mathrm{sup}})/(\text{operation hour}/36000)\eta_{\mathrm{elec}} \tag{8}$$

Table 4 shows the parameter used in the modeling of biomass.

E. VOLTAGE CONTROL FOR THE INVERTER PI CONTROLLER

The PI controller aims to regulate the inverter voltage control in this system. In the PI controller design, Clarke transformation and Park's transformation convert three-phase voltage and current from the power load variable as feedback signal to dq variable and vice versa as this equation [36];

$$P = 3/2(v_{\mathrm{od}} i_{\mathrm{od}} + v_{\mathrm{oq}} i_{\mathrm{oq}}) \tag{9}$$

$$q = 3/2(v_{\mathrm{oq}} i_{\mathrm{od}} + v_{\mathrm{od}} i_{\mathrm{oq}}) \tag{10}$$

The voltage V_d and V_q were compared with $V_{d\mathrm{ref}}$, 0 and angular frequency for processing in the PI controller to minimize the error. The equation involves [36];

$$\dot{\varphi_d} = \omega \mathrm{PLL} - \omega^*; \; i_{\mathrm{Id}}* = k_{\mathrm{iv},d}\varphi_d + k_{\mathrm{pv},d}\dot{\varphi_d} \tag{11}$$

$$\dot{\varphi_q} = v_{\mathrm{oq}} * - v_{\mathrm{oq}}; \; i_{\mathrm{Iq}}* = k_{\mathrm{iv},q}\varphi_q + k_{\mathrm{pv},q}\dot{\varphi_q} \tag{12}$$

Then, these signals are compared with I_d and I_q for PI controller processing. The equation involves;

$$\begin{aligned} \dot{\gamma_d} &= i_{\mathrm{Id}} * - i_{\mathrm{Id}}; \\ v_{\mathrm{id}}* &= -\omega_n L_f i_{\mathrm{Iq}} + k_{\mathrm{ic},d}\gamma_d + k_{\mathrm{pc},d}\dot{\gamma_d} \end{aligned} \tag{13}$$

$$\begin{aligned} \dot{\gamma_q} &= i_{\mathrm{Iq}} * - i_{\mathrm{Iq}}; \\ v_{\mathrm{iq}}* &= -\omega_n L_f i_{\mathrm{Id}} + k_{\mathrm{ic},q}\gamma_q + k_{\mathrm{pc},q}\dot{\gamma_q} \end{aligned} \tag{14}$$

Fig. 8 shows the feedback PI controller and Fig. 9 illustrates the PI controller block diagram for the inverter in MATLAB/Simulink PI controllers number one & three were for voltage controllers, and numbers two & four were for current controllers. Both current and voltage controller used feedback

signal from power load variable. The parameters involved in these PI controller is Proportional (P) and Integral(I). This research used a manual PI tuning method due to microgrid design complexity. The P and I parameters were tuned by try and error until the current and voltage graph was steady as shown in TABLE 5.

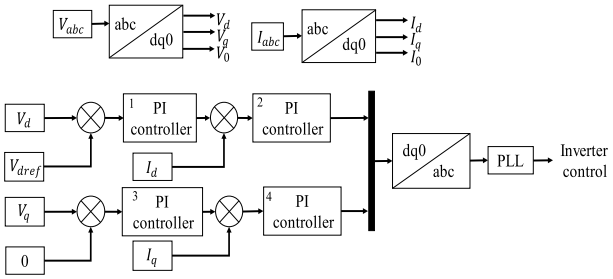

FIGURE 8. PI controller modeling [37].

TABLE 5. PI controller parameter.

Proportional, P		Integral, I	
1	3	2	4
1000	10e3	1e-6	1e-3

F. POWER HARMONIC FILTER MODELING

Power harmonic filter applied to reduce the voltage and THD percentage and harmonics during operation. In MATLAB/Simulink, the power harmonic filter was presented by RLC circuit. The equation involve is [31];

$$L_f = 0.1U^2/[2\pi f(P/3] \quad (15)$$

$$C_f = 0.05P/2\pi fU \quad (16)$$

where L_f is inductance filter, C_f is capacitance filter, U is inverter phase to phase voltage, f is frequency, and P is power output.

G. INTEGRATION OF HYBRID BM-SOLAR PV-WIND MICROGRID

The 100kW load connects with the 50kW solar, the 50kW wind, and the 0.8 MW biomass via an 11kV/240V step-down transformer. The integration of the hybrid BM-Solar PV-Wind is based on architecture in Fig. 1. Solar is connected to DC bus via boost converter and connected to AC via inverter with PI controller and power harmonic filter. Wind and biomass are directly connected to load through step-down transformer.

In the completed hybrid BM-PV-WT microgrid, the power output of each renewable energy is observed to ensure the validity of the simulation. Then, this research's voltage stability is determined by graph behavior, THD value of AC current, and voltage of each renewable energy. These outputs are measured using a three-phase voltage-current block diagram in Matlab/Simulink and THD measurement through FFT analysis.

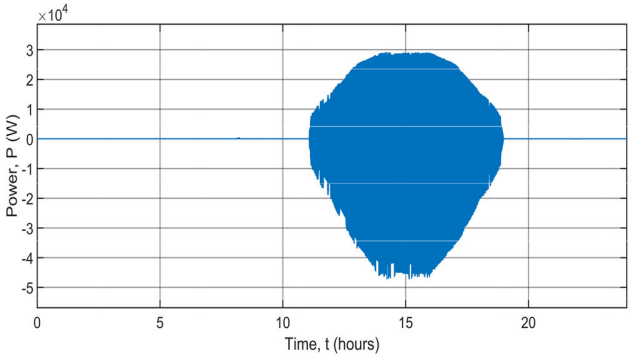

FIGURE 9. Solar PV power output.

III. RESULT & DISCUSSION

A. SOLAR PV

Fig. 9 illustrates the solar power output considering the Mersing solar temperature data. The graph shows that the solar panel expected to produce 29kW with an average temperature of 26 °C. The graph shows 0 W power output from 1 to 11 hours and 18 to 19 hours because the irradiance was 0 W/m^{2}as it was before the sunrise and after sunset. Therefore, solar need backs up at the night with other sources.

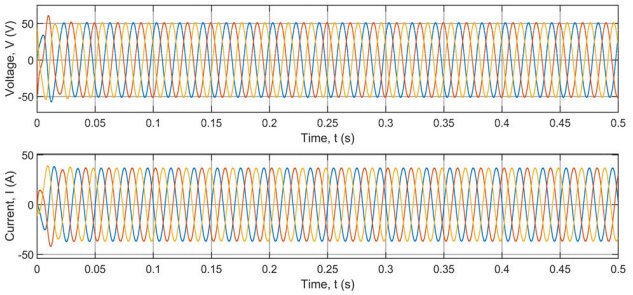

FIGURE 10. Simulated solar PV AC voltage and current.

Fig. 10 shows the result of the solar PV's AC voltage current after undergoing conversion from the DC bus. The graph depicts the initial voltage fluctuation caused by power electronics devices such as inductor and capacitor presence in the power system, taking advantage of the induced variation in voltage or current. Hence, the system requires time to stabilize. The THD value for solar AC voltage and current are 6.66% and 4.33%, respectively, as shown in Fig. 11. In the harmonic power system, if the system has below 10% THD value, the voltage and current are stable.

B. WIND

Fig. 12 illustrates that the wind's power output is an average of 20kW with variable wind speed varying between 1 m/s to 6 m/s throughout the year. The researcher in [12] has concluded that most of the places in Malaysia cannot generate power from the wind due to their geographical condition and low wind speed. However, the average power output of 20kW is relatively high for Malaysia because the actual data location was near the seashore and the usage of PMSG in the system.

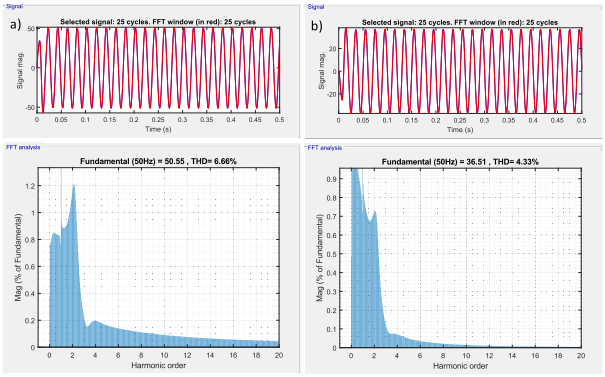

FIGURE 11. Solar THD a) voltage b) current.

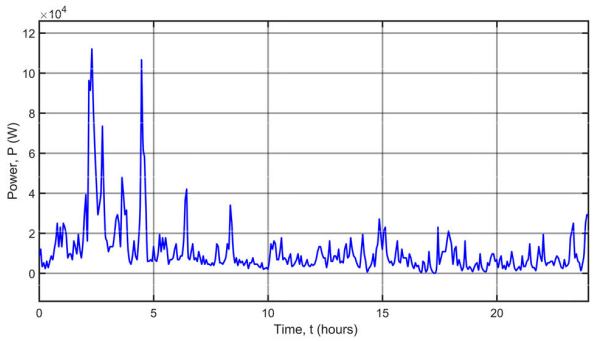

FIGURE 12. Wind power output.

The significant advantage of PMSG is to increase the wind turbine's reliability and optimal efficiency. As a result, the wind turbine's power output can be kept at high power.

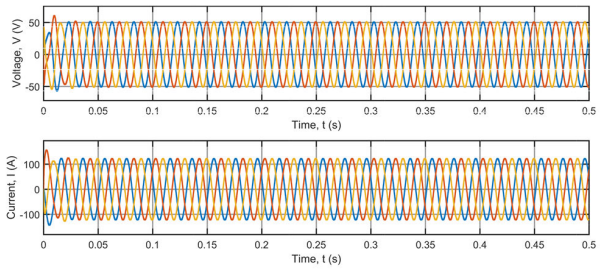

FIGURE 13. Simulated Wind AC voltage and current.

Next, the AC voltage and current illustrated in Fig. 13 exhibit the same behavior as AC voltage and current of the solar generation due to inductance and capacitance as a harmonic filter to reduce the THD value. The graph reaches steady state at 0.0429s for voltage and 0.0362s for current. The THD value for the wind AC voltage and current obtained was 6.66% and 2.53%, respectively, as shown in Fig. 14. The THD values approximates the solar AC voltage and current due to the direct connection between solar and wind before step-down to supply the load.

C. BIOMASS

This system's biomass power generation is based on [35] using a 9240 t/year amount of EFB. With this amount of EFB,

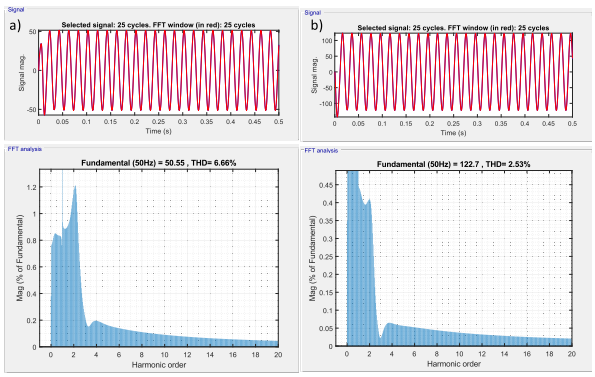

FIGURE 14. Wind THD a) voltage b) current.

the system targets generating 0.89 MW of power. However, due to power losses caused by the transmission line and power conversion from mechanical to electrical.

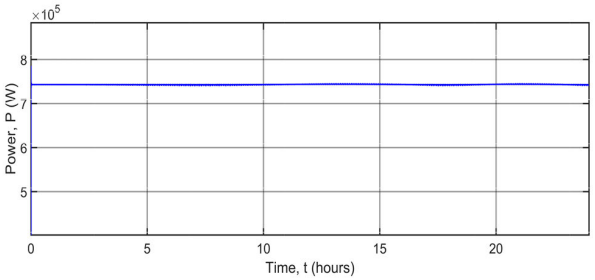

FIGURE 15. Biomass power output.

Thus, the electrical power obtained was 750kW, as shown in Fig 15. The power output of the biomass was constant throughout the simulation because the input database was not fluctuating as solar and wind. Nevertheless, the power output at the beginning of the simulation increased to 1200kW due to system instability caused by an electronic device such as a transformer.

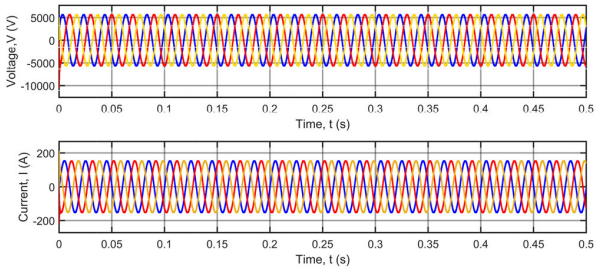

FIGURE 16. Simulated biomass AC voltage and current.

Moving to AC voltage and current observation, Fig. 16 illustrates the simulation result. The graph shows the sinusoidal pattern without any disturbance but only the beginning due to the exact cause with solar and wind. Therefore, the fundamental percentage of the third harmonic shown in Fig.17 increases abruptly. It also happened to all AC voltage and current of other RE sources, which shows an increasing percentage of fundamentals at the beginning of

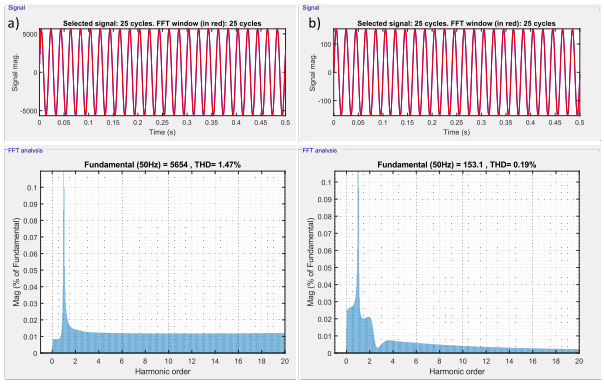

FIGURE 17. Biomass THD a) voltage b) current.

the simulation. Furthermore, the amount of AC voltage and current for biomass is relatively high compared with other RES as the generation scale is 750kW. Fig.17 shows the FFT analysis for biomass AC voltage and current. A THD of 1.47 % was reached for voltage and 0.15 % for current. The THD values are in allowable THD values in the power system to work without any power disturbance according to IEEE standard.

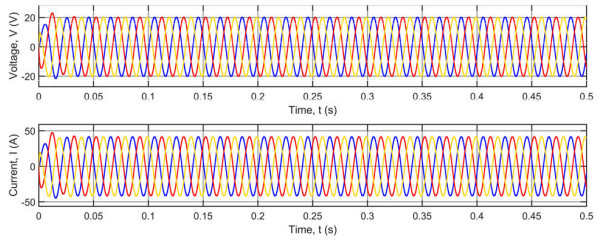

FIGURE 18. Simulated load AC voltage and current.

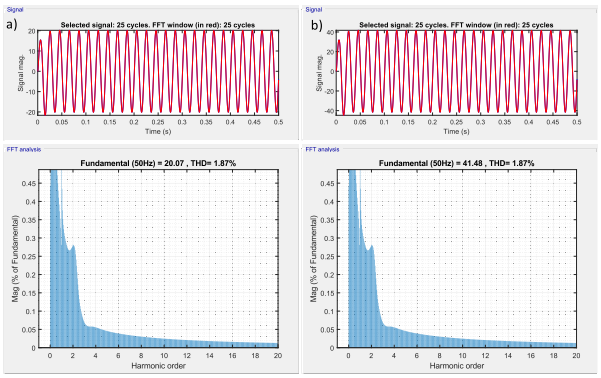

FIGURE 19. Load THD a) voltage b) current.

D. LOAD

Lastly, the load AC voltage and current also are monitored as this part is crucial in the power system as it is near the consumer. Fig. 18 shows the load AC voltage and current measurement after the 400V step-down transformer. The graph shows the sinusoidal pattern and fluctuates at the beginning of simulation for the same reason as solar, wind, and biomass. For the THD value, 1.87% is acquired for voltage and 1.87 % for current, as illustrated in Fig. 19. Increasing percentage of fundamentals at the beginning of the simulation happened due to fluctuating graph at the beginning before reaching at steady state. According to the primary electricity company in Malaysia, Tenaga Nasional Berhad (TNB), the acceptable permissible value of THD voltage at the point of common coupling (PCC) for 400 V distribution is less than 5% [38]. Besides that, this system is also suitable to inject into the primary grid to whether at transmission line or distribution line, as the THD is still in TNB acceptable permissible THD range.

TABLE 6 shows the result summary of this study. This table shows that all the RE sources and load THD values are in the acceptable range.

TABLE 6. Result summary.

Sources	Average Power	Voltage THD	Current THD
Solar	0.6kW	6.66%	4.33%
Wind	20kW	6.66%	2.53%
Biomass	750kW	1.47%	0.19%
load	-	1.87%	1.87%

TABLE 7. Result comparison from existing paper.

Ref	RE Sources	Method	Voltage THD (%)
This Study	BM-PV-Wind	PI	1.87
[39]	PV-Wind	MPC	1.05
[40]	PV-Wind	Repetitive and state feedback control	1.30
[41]	PV-Wind	Voltage Source Converter (VSC)	3.80
[42]	PV	Proportional Resonance (PR) and Predictive Current (PC)	3.15
[39]	PV-wind	PI	3.20

To verify this study, the THD voltage result was compared with a similar approach from existing research in TABLE 7. However, none of these earlier studies integrated BM, PV, and wind in the microgrid system. From this table, it can be concluded that MPC has the lowest voltage THD value compared to others. Even so, this study reached quite a similar voltage THD value to other methods, with a difference of 0.85% from the MPC method. For similar voltage method comparison with [39], this study has better THD voltage value.

IV. CONCLUSION

This paper has presented an integration of RE in an off-grid connected microgrid for Malaysia's actual data from Mersing in 2018, and the input data received from MMD. The RE microgrid integration includes solar photovoltaic, wind, and biomass. Combining these RE in the system can back up each

other as biomass input is not intermittent. The average power output of solar, wind, and biomass were 60kW, 20kW, and 750kW, respectively. Not only focus on RE integration, but this paper also focuses on the voltage control of the system. PI controller is implemented in the system by manually tuning the PI parameter. THD value of the AC voltage and current of each RE and load are watched to ensure system stability. As a result, the voltage THD value of all RE and load are 6.66%, 6.66%, 1.47%, and 1.87%, respectively, were in acceptable permissible range by TNB standard harmonic. As well as that, this system also can be injected into the primary grid for the grid-connected microgrid. The paper's primary contribution is the integration of multiple renewable energy research that manages to control the system's voltage that can be supplied to any type of load demand such as industry and household by only adjusting the voltage control parameter.

For future recommendations, an automatically tuning PI parameter with a dynamic load application can be performed to ease the voltage control in the system. With this implementation, the hybrid BM-PV-wind system can fulfill load demand. Furthermore, an Energy Storage System (ESS) also needs to be considered in the future, especially for off-grid connected microgrids, for a realistic result. Lastly, a detailed feasibility study for this system must also be considered to ensure this hybrid RE microgrid is economically friendly.

ACKNOWLEDGMENT

The authors would like to thank the Malaysia Meteorological Department (MMD) for supplying solar irradiance and wind speed data.

REFERENCES

[1] *NASA: Climate Change and Global Warming*. Accessed: Dec. 9, 2021. [Online]. Available: https://climate.nasa.gov/

[2] A. Khatibzadeh, M. Besmi, A. Mahabadi, and M. R. Haghifam, "Multi-agent-based controller for voltage enhancement in AC/DC hybrid microgrid using energy storages," *Energies*, vol. 10, no. 2, p. 169, Feb. 2017, doi: 10.3390/en10020169.

[3] Q. Tabart, I. Vechiu, A. Etxeberria, and S. Bacha, "Hybrid energy storage system microgrids integration for power quality improvement using four-leg three-level NPC inverter and second-order sliding mode control," *IEEE Trans. Ind. Electron.*, vol. 65, no. 1, pp. 424–435, Jan. 2018, doi: 10.1109/TIE.2017.2723863.

[4] J. Kumar, A. Agarwal, and N. Singh, "Design, operation and control of a vast DC microgrid for integration of renewable energy sources," *Renew. Energy Focus*, vol. 34, pp. 17–36, Sep. 2020, doi: 10.1016/j.ref.2020.05.001.

[5] S. H. Badruhisham, M. S. A. Hanifah, S. H. Yusoff, N. F. Hasbullah, and M. Yaacob, "Integration of hybrid biomass-solar photovoltaic-wind turbine in microgrid application," in *Proc. 8th Int. Conf. Comput. Commun. Eng. (ICCCE)*, Jun. 2021, pp. 87–92.

[6] M. Ahmed, L. Meegahapola, A. Vahidnia, and M. Datta, "Stability and control aspects of microgrid architectures—A comprehensive review," *IEEE Access*, vol. 8, pp. 144730–144766, 2020, doi: 10.1109/ACCESS.2020.3014977.

[7] V. Nasirian, Q. Shafiee, J. M. Guerrero, F. L. Lewis, and A. Davoudi, "Droop-free distributed control for AC microgrids," *IEEE Trans. Power Electron.*, vol. 31, no. 2, pp. 1600–1617, Feb. 2016, doi: 10.1109/TPEL.2015.2414457.

[8] M. I. Nazir, I. Hussain, A. Ahmad, I. Khan, and A. Mallik, "System modeling and reliability assessment of microgrids: A review," *Sustainability*, vol. 14, no. 1, pp. 1–33, 2022, doi: 10.3390/su14010126.

[9] S. Abhinav, H. Modares, F. L. Lewis, and A. Davoudi, "Resilient cooperative control of DC microgrids," *IEEE Trans. Smart Grid*, vol. 10, no. 1, pp. 1083–1085, Jan. 2019., doi: 10.1109/TSG.2018.2872252.

[10] S. Parhizi, H. Lotfi, A. Khodaei, and S. Bahramirad, "State of the art in research on microgrids: A review," *IEEE Access*, vol. 3, pp. 890–925, 2015 doi: 10.1109/ACCESS.2015.2443119.

[11] A. Hirsch, Y. Parag, and J. Guerrero, "Microgrids: A review of technologies, key drivers, and outstanding issues," *Renew. Sustain. Energy Rev.*, vol. 90, pp. 402–411, Jul. 2018, doi: 10.1016/j.rser.2018.03.040.

[12] W. S. W. Abdullah, M. Osman, M. Z. A. A. Kadir, and R. Verayiah, "The potential and status of renewable energy development in Malaysia," *Energies*, vol. 12, no. 12, p. 2437, Jun. 2019, doi: 10.3390/en12122437.

[13] F. R. Badal, P. Das, S. K. Sarker, and S. K. Das, "A survey on control issues in renewable energy integration and microgrid," *Protection Control Mod. Power Syst.*, vol. 4, no. 1, p. 8, Dec. 2019, doi: 10.1186/s41601-019-0122-8.

[14] M. H. Saeed, W. Fangzong, B. A. Kalwar, and S. Iqbal, "A review on microgrids' challenges & perspectives," *IEEE Access*, vol. 9, pp. 166502–166517, 2021, doi: 10.1109/access.2021.3135083.

[15] A. Hossain Bagdadee and L. Zhang, "Power quality improvement provide digital economy by the smart grid," *IOP Conf. Ser., Mater. Sci. Eng.*, vol. 561, no. 1, Oct. 2019, Art. no. 012097, doi: 10.1088/1757-899X/561/1/012097.

[16] J. Lai, J. Liu, J. Su, Y. Shi, X. Yang, and T. Xie, "Fast voltage balance control strategy of microgrid inverter operating in islanded mode," in *Proc. IEEE Int. Power Electron. Appl. Conf. Expo. (PEAC)*, Nov. 2018, pp. 1–5, doi: 10.1109/PEAC.2018.8590373.

[17] C. Tu, F. Xiao, Q. Guo, and Z. Lan, "High voltage quality control strategy of microgrid main inverter for islanded microgrid," in *Proc. IEEE Int. Power Electron. Appl. Conf. Expo. (PEAC)*, Nov. 2018 vol. 1, no. 1, pp. 1–5, doi: 10.1109/PEAC.2018.8590352.

[18] S. K. Sarkar, F. R. Badal, S. K. Das, and Y. Miao, "Discrete time model predictive controller design for voltage control of an islanded microgrid," in *Proc. 3rd Int. Conf. Electr. Inf. Commun. Technol. (EICT)*, Dec. 2017, pp. 1–6, doi: 10.1109/EICT.2017.8275162.

[19] M. Dai, M. N. Marwali, J.-W. Jung, and A. Keyhani, "A three-phase four-wire inverter control technique for a single distributed generation unit in island mode," *IEEE Trans. Power Electron.*, vol. 23, no. 1, pp. 322–331, Jan. 2008, doi: 10.1109/TPEL.2007.911816.

[20] S. Kirmani, M. Jamil, and I. Akhtar, "Bi-directional power control mechanism for a microgrid hybrid energy system with power quality enhancement capabilities," *Int. J. Renew. Energy Res.*, vol. 7, no. 4, pp. 1962–1969, Dec. 2017.

[21] S. Singh, M. Singh, and S. C. Kaushik, "Feasibility study of an islanded microgrid in rural area consisting of PV, wind, biomass and battery energy storage system," *Energy Convers. Manage.*, vol. 128, pp. 178–190, Nov. 2016, doi: 10.1016/j.enconman.2016.09.046.

[22] K. Sundaramoorthy and A. Sankar, "Performance evaluation of a control strategy developed for a hybrid energy system integrated in DC–AC microgrids," *Electr. Power Compon. Syst.*, vol. 42, no. 15, pp. 1762–1770, Nov. 2014, doi: 10.1080/15325008.2014.949914.

[23] P. Balamurugan, S. Ashok, and T. L. Jose, "Optimal operation of biomass/wind/PV hybrid energy system for rural areas," *Int. J. Green Energy*, vol. 6, no. 1, pp. 104–116, Mar. 2009, doi: 10.1080/15435070802701892.

[24] M. W. Rahman, M. S. Hossain, A. Aziz, and F. M. Mohammedy, "Prospect of decentralized hybrid power generation in Bangladesh using biomass, solar PV & wind," in *Proc. 3rd Int. Conf. Develop. Renew. Energy Technol. (ICDRET)*, May 2014, pp. 2–7, doi: 10.1109/icdret.2014.6861690.

[25] M. U. Khan, M. Hassan, M. H. Nawaz, M. Ali, and R. Wazir, "Techno-economic analysis of PV/wind/biomass/biogas hybrid system for remote area electrification of southern Punjab (Multan), Pakistan using Homer pro," in *Proc. Int. Conf. Power Gener. Syst. Renew. Energy Technol. (PGSRET)*, Sep. 2018, pp. 10–12, doi: 10.1109/PGSRET.2018.8686032.

[26] T. Som and N. Chakraborty, "Economic feasibility studies on wind-biomass-solar based microgid power system through a modified differential evolution technique," in *Proc. IET 4th Int. Conf. Sustain. Energy Intell. Syst. (SEISCON)*, Chennai, India, Dec. 2013, pp. 20–28, doi: 10.1049/ic.2013.0289.

[27] A. D. Dhass and S. Harikrishnan, "Cost effective hybrid energy system employing solar-wind-biomass resources for rural electrification," *Int. J. Renew. Energy Res.*, vol. 3, no. 1, pp. 222–229, 2013.

[28] *Pejabat Meteorologi Mersing—Google Maps*. Accessed: Apr. 18, 2022. [Online]. Available: https://www.google.com.my/maps/place/Pejabat+Meteorologi+Mersing/2.4451463,103.828927,17z/data=!3m1!4b1!4m5!3m4!1s0x31c54b9ba081d869:0xafefa26012ab8672!8m2!3d2.4451322!4d103.8311945
[29] *MetMalaysia: Utama*. Accessed: Apr. 18, 2022. [Online]. Available: https://www.met.gov.my/
[30] O. Ibrahim, N. Z. Yahaya, N. Saad, and M. W. Umar, "MATLAB/simulink model of solar PV array with perturb and observe MPPT for maximising PV array efficiency," in *Proc. IEEE Conf. Energy Convers. (CENCON)*, Oct. 2015, pp. 254–258, doi: 10.1109/CENCON.2015.7409549.
[31] N. Guler and E. Irmak, "MPPT based model predictive control of grid connected inverter for PV systems," in *Proc. 8th Int. Conf. Renew. Energy Res. Appl. (ICRERA)*, Nov. 2019, pp. 982–986, doi: 10.1109/ICRERA47325.2019.8997105.
[32] M. Kamran, M. Mudassar, M. R. Fazal, M. U. Asghar, M. Bilal, and R. Asghar, "Implementation of improved perturb & observe MPPT technique with confined search space for standalone photovoltaic system," *J. King Saud Univ., Eng. Sci.*, vol. 32, no. 7, pp. 432–441, 2020, doi: 10.1016/j.jksues.2018.04.006.
[33] Y. Errami, M. Ouassaid, and M. Maaroufi, "Optimal power control strategy of maximizing wind energy tracking and different operating conditions for permanent magnet synchronous generator wind farm," *Energy Proc.*, vol. 74, pp. 477–490, Aug. 2015, doi: 10.1016/j.egypro.2015.07.732.
[34] R. Ben Ali, H. Schulte, and A. Mami, "Wind Turbine system based on PMSG generator," in *Proc. Evolving Adapt. Intell. Syst. (EAIS)*, May 2017, pp. 1–6.
[35] I. F. M. Jaye, "Renewable, local electricity generation from palm oil mill residues: A case study from Peninsular Malaysia," Univ. Surrey, Guildford, U.K., Tech. Rep. 2315244125, Feb. 2019, pp. 1–289. [Online]. Available: https://openresearch.surrey.ac.uk/esploro/outputs/doctoral/Renewable-local-electricity-generation-from-palm/99513007502346#file-0
[36] M. Rasheduzzaman, J. A. Mueller, and J. W. Kimball, "An accurate small-signal model of inverter-dominated islanded microgrids using (DQ) reference frame," *IEEE J. Emerg. Sel. Topics Power Electron.*, vol. 2, no. 4, pp. 1070–1080, Jul. 2014, doi: 10.1109/JESTPE.2014.2338131.
[37] I. Alhamrouni, M. A. Hairullah, N. S. Omar, M. Salem, A. Jusoh, and T. Sutikno, "Modelling and design of PID controller for voltage control of AC hybrid micro-grid," *Int. J. Power Electron. Drive Syst.*, vol. 10, no. 1, pp. 151–159, Mar. 2019, doi: 10.11591/ijeecs.v15.i2.pp581-592.
[38] TNB. (2001). *Supply Application Handbook*. [Online]. Available: https://www.mytnb.com.my/themes/user/mytnb/pdf/2019_ESAH_Complete_v3.1.pdf
[39] Y. Shan, J. Hu, K. W. Chan, Q. Fu, and J. M. Guerrero, "Model predictive control of bidirectional DC–DC converters and AC/DC interlinking converters—A new control method for PV-wind-battery microgrids," *IEEE Trans. Sustain. Energy*, vol. 10, no. 4, pp. 1823–1833, Oct. 2019, doi: 10.1109/TSTE.2018.2873390.
[40] W. Ma and S. Ouyang, "Control strategy for inverters in microgrid based on repetitive and state feedback control," *Int. J. Electr. Power Energy Syst.*, vol. 111, pp. 447–458, Oct. 2019, doi: 10.1016/j.ijepes.2019.04.002.
[41] I. Alhamrouni, W. Wahab, M. Salem, N. H. A. Rahman, and L. Awalin, "Modeling of micro-grid with the consideration of total harmonic distortion analysis," *Indones. J. Electr. Eng. Comput. Sci.*, vol. 15, no. 2, pp. 581–592, 2019, doi: 10.11591/ijeecs.v15.i2.pp581-592.
[42] X.-H. Guo, C.-W. Chang, and L.-R. Chang-Chien, "Digital implementation of harmonic and unbalanced load compensation for voltage source inverter to operate in grid forming microgrid," *Electronics*, vol. 11, no. 6, p. 886, Mar. 2022.

SAIDATUL HANEEN BADRUHISHAM received the bachelor's degree in mechanical engineering from Universiti Tenaga Nasional (UNITEN). She is currently pursuing the master's degree in electronic engineering with International Islamic University Malaysia (IIUM). Her current research interest includes renewable energy microgrid.

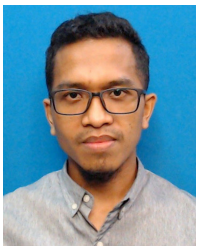

MOHD SHAHRIN ABU HANIFAH (Member, IEEE) received the Master of Engineering and Doctor of Engineering degrees from Tokai University, Kanagawa, Japan, in 2012 and 2016, respectively. He is currently an Assistant Professor with the Department of Electrical and Computer Engineering, International Islamic University Malaysia, Gombak. He is teaching programming for engineers and engineering electromagnetics courses. His research interests include power distribution network reconfiguration, service restoration optimization using a multi-objectives algorithm, electric vehicle charging station integration in the distribution networks, and application of distributed generation and renewable energy in microgrid.

SITI HAJAR YUSOFF (Member, IEEE) received the M.Eng. degree (Hons.) in electrical engineering and the Ph.D. degree in electrical engineering from the University of Nottingham, U.K., in 2009 and 2014, respectively. In 2015, she became an Assistant Professor with the Department of Electrical and Computer Engineering, International Islamic University Malaysia, Gombak. She is currently a Lecturer in control of power electronics and electrical power systems. Her research interests include controlling power converters and drives, matrix and multilevel converters, the IoT, smart meter, wireless power transfer for dynamic charging in electric vehicles (EVs), and renewable energy.

NURUL FADZLIN HASBULLAH received the Bachelor of Engineering degree (Hons.) from Cardiff University, Wales, in 2001, and the Ph.D. degree from The University of Sheffield, U.K., in 2010, researching the electrical and optical characteristics of quantum dot laser structures. Later, she worked as an Integrated Chip Design Engineer at Malaysia Microelectronics Solution, Cyberjaya, for a year, before joining academia, teaching at University Tenaga Nasional, Bangi, Malaysia, as a Tutor. In 2003, she moved to International Islamic University Malaysia as an Assistant Lecturer. She is currently a Professor at the Department of Electrical and Computer Engineering, Faculty of Engineering. Her research interests include semiconductor device characterization, optical detectors, and hard radiation devices.

MASHKURI YAACOB (Life Senior Member, IEEE) received the Bachelor of Engineering degree from the University of New South Wales, Australia, and the M.Sc. and Ph.D. degrees from Manchester, U.K. He was the Third Vice-Chancellor of Universiti Tenaga Nasional (UNITEN), Putrajaya, Malaysia, from 2007 to 2014. Previously, he was the Deputy Vice-Chancellor (Academic) of the University of Malaya (UM), Kuala Lumpur, where he began his academic career as a Lecturer and retired as a Senior Professor. He was the Chairperson of the Institution of Engineering and Technology (IET) (U.K.) Malaysia Branch and a Council Member of the IET, London, from 2003 to 2005. He was the Founding Dean of the Computer Science and IT Faculty, UM. He started the publication of the *Malaysian Journal of Computer Science*, in 1986, which has currently received the web of science recognition. As the Vice-Chancellor of UNITEN, he has played a significant role in the growth of the university, particularly in rebranding the university as a quality Private University in Malaysia. UNITEN won the coveted Prime Minister's Industry Quality Excellence Award, in 2009, the International Asia Pacific Quality Award 2010 for Education, and the International Crown Quality Award 2010 for Education (London). He is currently a Professor at the Kulliyyah of Engineering, International Islamic University Malaysia. His research interests include computer system architecture, digital filters, VLSI design, power electronics, and renewable energy resources.